Fibers and Polymers 2021, Vol.22, No.1, 285-293
DOI 10.1007/s12221-021-9155-5

ISSN 1229-9197 (print version)
ISSN 1875-0052 (electronic version)

Effect of Process Parameters on Fiber Diameter and Fiber Distribution of Melt-Blown Polypropylene Microfibers Produced by Biax Line

Numan Hoda[1]*, Firdevs Mert[2], Fatma Kara[3], Hande Gul Atasagun[4], and Gajanan S Bhat[5]

[1]*Department of Material Science and Engineering, Akdeniz University, Antalya 07058, Turkey*
[2]*Department of Basic Pharmaceutical Sciences, Faculty of Pharmacy, Suleyman Demirel University, Isparta 32200, Turkey*
[3]*Department of Chemistry, Akdeniz University, Antalya 07058, Turkey*
[4]*Department of Textile, Clothing, Shoes and Leather, Izmir Vocational School, Dokuz Eylul University, Izmir 35380, Turkey*
[5]*Department of Textiles, Merchandising, and Interiors, University of Georgia, Athens, GA 30602, USA*
(Received November 1, 2019; Revised April 13, 2020; Accepted April 16, 2020)

Abstract: Meltblown nonwovens market has been continuing to grow because of the unique characteristics of allowing the production of microfiber webs directly from a thermoplastic polymer in a single step. Whereas a vast majority of meltblown processes have utilized the traditional Exxon die, the Biax-die has also been used in some processes. The aim of this study was to understand the effect of critical process conditions of the Biax process, which has the advantage of lower high pressure hot air consumption compared to the traditional process, on the structure of meltblown webs. As the performance properties of meltblown nonwovens are mainly determined by the fiber diameter and diameter distribution, this study focused on these two characteristics considering various process conditions such as melt temperature, melt throughput, air temperature and air pressure. In conclusion, it was observed that there were three distribution types, the normal distribution, log-normal distribution, and skewed log-normal distribution, for meltblown webs produced by the Biax process. Air pressure and melt throughput were the most effective process conditions on the fiber diameter of meltblown polypropylene webs. It was also observed that fine fiber webs close to one-micron average fiber diameter and relatively narrower fiber diameter distribution can be produced under appropriate processing conditions using the Biax process.

Keywords: Biax die, Melt blowing, Polypropylene, Nonwovens, Fiber diameter

Introduction

Melt blowing is a one-step process used extensively to manufacture microfibers from polymers. The fibers produced by melt blowing may have a diameter as fine as 0.1 μm; however, it usually varies between 2-5 μm [1,2]. Nonwovens produced from these microfibers have a high surface area per unit weight, self-bonding ability, and good insulation and barrier characteristics [3]. Due to the desirable properties, these nonwovens are widely used to produce high-quality filtration materials, thermal insulation materials, medical supplies, and garments.

In the melt blowing process, extruder melts the thermoplastic resin, and the molten resin is forced through a melt-blowing die. The typical melt blowing die consists of a row of orifices in which molten polymer flows out forming fibers, and high-velocity hot air jets thin down these fibers. The formed continuous fibers are collected as a nonwoven web on a moving collector [4,5]. The melt blowing process is categorized as Exxon or Biax/Schwarz according to the spinnerette or die designs used. The Exxon and Biax/Schwarz die models are shown in Figures 1(a) and (b), respectively. The Exxon die is a single-row-hole type consisting of drilled holes with two air knives at both sides (Figure 2(a)). On the other hand, the Biax/Schwarz design has multiple-rows of polymer nozzles and square or triangular air holes surrounding these nozzles, as shown in Figure 2(b), which provide a uniform stream of attenuating air to each nozzle [6-8]. The Biax die enables high melt viscosity polymers, which require higher melt pressure during melt blowing, to be processed [7,9]. The multi-row Schwarz die design has the ability to manufacture more fibers per die length as compared to single-row Exxon die [10]. In addition, parallel plate die design is more cost-effective compared to conventional Exxon slot melt blowing die, under similar operation conditions [8].

The melt-blown fiber diameters and their distribution can be affected by the die design, as well as process conditions such as die-to-collector distance (DCD), polymer throughput

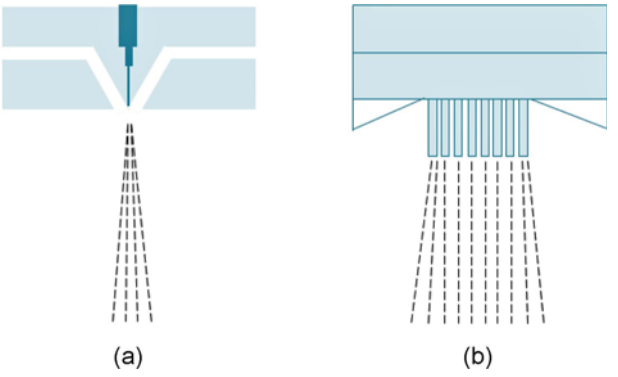

Figure 1. Side views of (a) Exxon and (b) Biax/Schwarz die designs [7].

*Corresponding author: nhoda@akdeniz.edu.tr

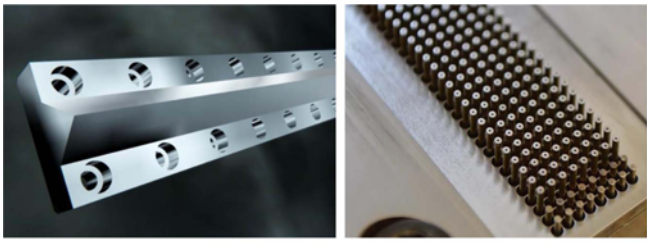

Figure 2. Cross sections of (a) Exxon die and (b) Biax die designs [11,12].

rate, processing temperatures, air pressure/airflow rate, collector drum speed, and collector vacuum [3,9,15-19]. Therefore, it is possible to manufacture nonwovens or microfibers with desired properties by changing these parameters during melt-blowing. The fiber diameter is inversely proportional to the processing temperature because higher temperatures influence the polymer viscosity, attenuation process, and fiber entanglement at places not near the die [15,20-22]. Decreasing polymer mass flow rate leads to a reduction of fiber diameter due to the fact that the drag force from the air jet is acting on a lower polymer mass [3,15,23]. Moreover, fiber diameter reduces with an increase in airflow rates because of the same dragging force generated by the attenuation air [15,20,23]. Duran *et al.* [17] examined the effect of collector drum speed and vacuum and air pressure on the fiber diameter of polypropylene melt-blown nonwovens. They indicated that increases in collector drum speed and die air pressure and the decrease in collector vacuum allowed the production of finer fibers. Similarly, Han *et al.* [24] stated that the diameter of polypropylene fibers was smaller and more uniform at higher air pressures based on the findings of a study where they used two dies having different numbers of orifices per centimeter. Changing the DCD also will affect the fiber diameter because polymer melt transits from the viscous state to the crystalline state when the melt temperature reduces slowly from the die to the collector [25-28]. Yesil and Bhat [18] investigated the fiber diameter of polyethylene used in melt-blown nonwovens and reported that their average fiber diameter decreased with increasing DCD and die temperature. Also, it was observed that while finer fibers were produced as a result of an increase in air pressure from 20 to 35 kPa, the fiber diameter did not decrease any more above 35 kPa. Chen *et al.* [14,29,30] predicted the fiber diameter of melt-blown nonwovens by using the combination of two models they established and examined the effect of process conditions on the fiber diameter. They claimed that finer fibers resulted from a lower polymer flow rate and higher initial polymer temperature, initial air velocity, and polymer melt flow index. Pu *et al.* [31] used an electrostatic-assisted melt-blown system to produce polypropylene fibers and observed that when the voltage increased from 0 to 40 kV under a fixed electric field distance of 20 cm, average fiber diameter decreased, and the uniformity of the diameter was much better.

Whereas a majority of the researches in the literature has been conducted on the melt blowing process using the Exxon type dies, there are a limited number of studies using the Biax process that is considered more efficient [9,10,17, 19,32-34]. The Biax type die, due to its unique design, offers advantages to the process with relatively lower air consumption, and thus lower cost since the major cost of the process is from energy used due to a large volume of high pressure hot air [30]. Therefore, this study was conducted to examine the impact of various process parameters, such as extruder and die temperatures, screw speed, air pressure, and air temperature on the fiber diameter and its distribution. The findings of this study can contribute to the design of better melt-blown nonwovens using an economical process for filter media and thermal and acoustic insulation materials.

Experimental

In this study, commercially available polypropylene resin (LG Chem, South Korea), which has a relative density of 0.9 g/cm^3 (20 °C) and melt flow rate (MFR) of 1200 g/ 10 min, was used during the melt blowing process. This process was conducted using the 380 mm Biax melt-blown pilot line system that is equipped with a spinneret, which has 720 nozzles with a diameter of 150 μm (0.006") ID in 4 rows with air curtains. The collector speed and distance between the nozzle and collector were kept constant as 20 m/min and 25 cm, respectively.

To systematically examine the influence of process parameters, screw speed, temperatures (i.e., Zone 1, 2, and 3 in the extruder, clamp, die, and air) and air pressure were carefully varied during the production process, keeping all other parameters same. A total of 60 samples were produced at three different air pressures (35, 69, and 103 kPa), four different screw speeds (20, 30, 40, and 50 rpm), and five different temperatures. Table 1 shows the design of experiments consisting of five groups of 12 samples each. Scanning electron microscope (SEM) images of some samples are given in Figures 3(a-b).

The diameters of at least 200 fibers were measured for each of the 60 samples produced in the melt blowing process from images taken using a polarization microscope (Leica DM750 P, Leica Microsystems, Wetzlar, Germany). The fiber diameter distributions were determined using Origin2019b data processing software (OriginLab Inc., USA). Goodness-of-fit was evaluated using the Kolmogorov-Smirnov and the Anderson-Darling tests at 1 %, 2 %, and 5 % significance levels (α) for normal and log-normal distributions. The normal probability distribution has a bell-shaped and

Table 1. Processing conditions of polypropylene melt-blown nonwovens

Set	Sample code	Screw speed (rpm)	Air pressure (kPa)	Temperatures (°C)					
				Zone			Clamp	Die	Air
				1	2	3			
Group 1	P1	20	35	165	175	190	190	190	170
	P2		69						
	P3		103						
	P4	30	35						
	P5		69						
	P6		103						
	P7	40	35						
	P8		69						
	P9		103						
	P10	50	35						
	P11		69						
	P12		103						
Group 2	P13	20	35	175	185	200	200	200	180
	P14		69						
	P15		103						
	P16	30	35						
	P17		69						
	P18		103						
	P19	40	35						
	P20		69						
	P21		103						
	P22	50	35						
	P23		69						
	P24		103						
Group 3	P25	20	35	185	195	210	210	210	190
	P26		69						
	P27		103						
	P28	30	35						
	P29		69						
	P30		103						
	P31	40	35						
	P32		69						
	P33		103						
	P34	50	35						
	P35		69						
	P36		103						
Group 4	P37	20	35	195	205	220	220	220	200
	P38		69						
	P39		103						
	P40	30	35						
	P41		69						
	P42		103						
	P43	40	35						
	P44		69						
	P45		103						
	P46	50	35						
	P47		69						
	P48		103						

Table 1. Continued

Set	Sample code	Screw speed (rpm)	Air pressure (kPa)	Temperatures (°C)					
				Zone			Clamp	Die	Air
				1	2	3			
Group 5	P49	20	35	205	215	230	230	230	210
	P50		69						
	P51		103						
	P52	30	35						
	P53		69						
	P54		103						
	P55	40	35						
	P56		69						
	P57		103						
	P58	50	35						
	P59		69						
	P60		103						

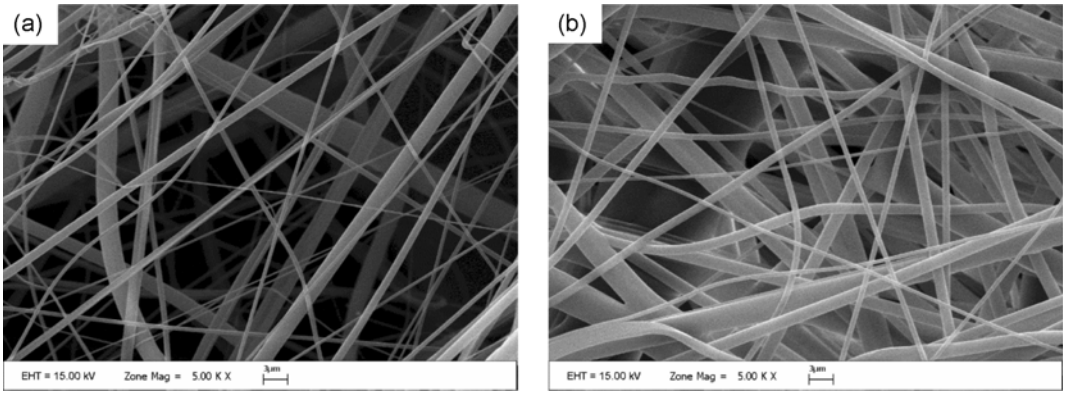

Figure 3. SEM images of meltblown samples coded (a) P51 and (b) P54.

symmetrical curve. The probability density function of a normal random variable X with mean μ and variance σ^2 is shown below [35,36],

$$f(x) = \frac{1}{\sigma\sqrt{2\pi}}\exp\left[-\frac{(x-\mu)^2}{2\sigma^2}\right] \text{ for } -\infty < x < \infty \quad (1)$$

The log-normal distribution, which can be commonly observed for meltblown structures, is based on the normal distribution. If Y=ln(x), and Y follows a normal distribution with mean μ and variance σ^2, it can be said that the positive random variable X is log-normally distributed [36,37]. The lognormal probability density function of X is given by,

$$f(x) = \frac{1}{\sqrt{2\pi}\sigma x}\exp\left[-\frac{(\ln x-\mu)^2}{2\sigma^2}\right] \text{ for } x > 0 \quad (2)$$

When the dataset obtained from this study did not follow normal or log-normal distribution as a result of the goodness-of-fit tests, the W value of the Shapiro Wilk test was calculated for these data. When this value was less than 0.8 for available data and more than 0.8 for log-transformed data, the distribution was called as skewed log-normal distribution [34].

Results and Discussion

Mean Fiber Diameter

Almost all of the performance characteristics of meltblown nonwovens (e.g., filtration efficiency, absorbency, and acoustic insulation) are mainly related to fiber diameter and its distribution due to increased surface area and porosity of the webs. Therefore, in this study, fiber diameter and their distribution were determined using high-resolution optical microscope images. Figures 4(a-e) illustrate the mean fiber diameters of polypropylene microfibers produced at different air pressures, screw speeds, and temperatures. The results demonstrated that while the mean fiber diameter varied from 1.1 μm to 4.2 μm, their standard deviation was in the range of 0.6 and 1.7 for all groups examined. The fiber diameter of webs in each group reduced when the air pressure increased from 35 kPa to 103 kPa. At higher air

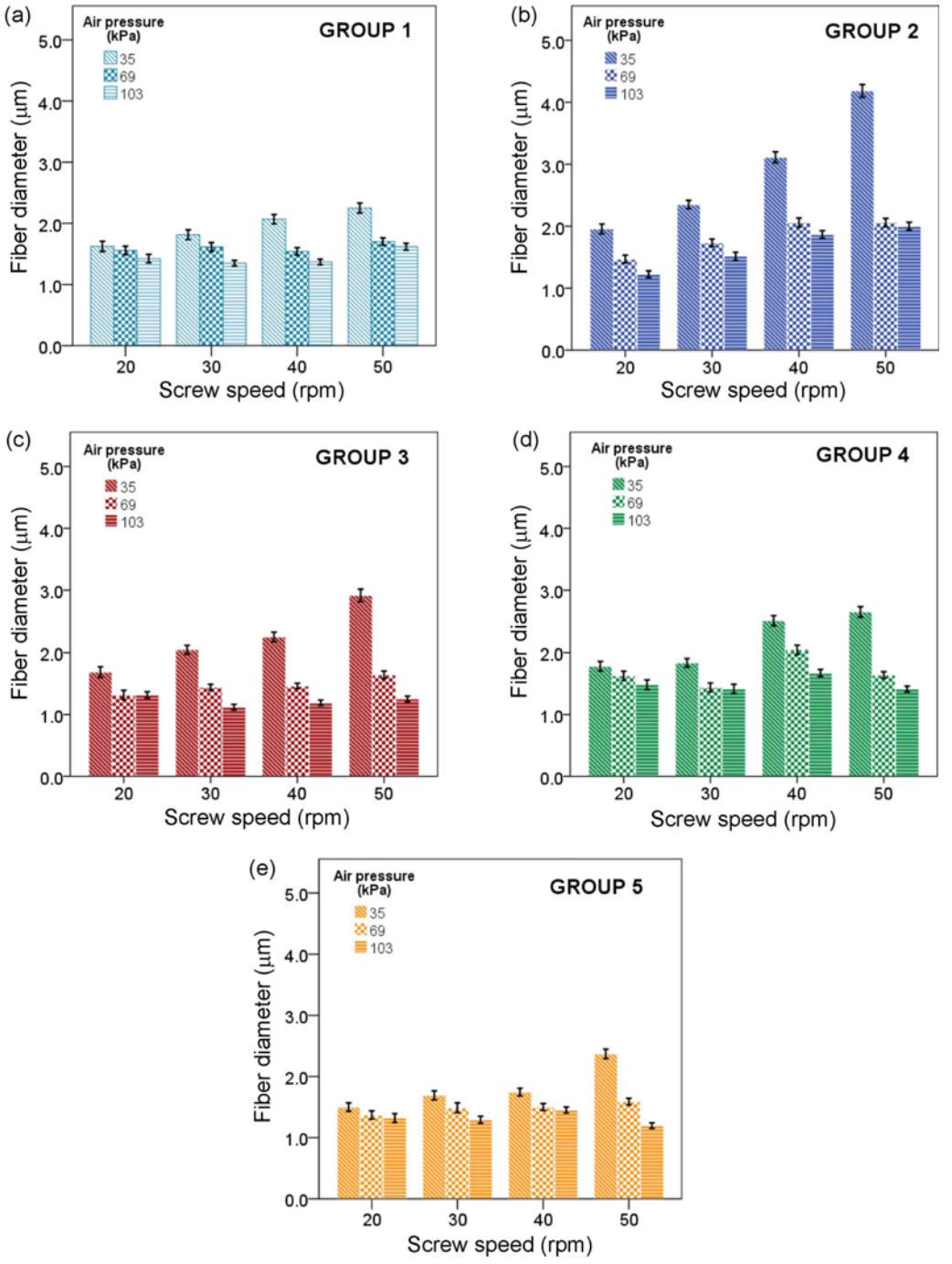

Figure 4. Mean fiber diameter produced polypropylene microfibers according to different temperatures. Data were presented as mean values with error bars indicating 1 standard error.

pressures, air speed increases, and consequently, finer fibers can be produced due to higher air drag force near the die, which is consistent with earlier findings [2,18,24].

As can be seen from the data in Figure 4, the fiber diameter of melt-blown fibers showed an increase as a result of increase in the screw speed. This increase was more apparent in all groups at 35 kPa air pressure. The increasing screw speed results in an increase in the melt throughput, which reduces the actual air to polymer ratio and the drafting force on the unit polymer mass. As a result, fiber diameter stays larger, owing to less effective drawing and attenuation. This finding is in accordance with the results of other studies [27,38]. Fiber diameter is affected by the increase in process temperatures during melt blowing. Overall, there is a slight

decrease in fiber diameter with increase in melt temperature. It is understood that the increase in the melt temperature reduces the fiber diameters because higher melt temperature leads to lower melt viscosity allowing easier elongation and stretching during fiber formation [21,27]. On the other hand, under certain conditions, lower viscosity might cause smaller drawing force in the fiber line, and accordingly non-effective drawing. Although there was an overall decrease in fiber diameter with increase in process temperatures, the trend was not always consistent (from Group 1 to 5) due to some outliers. For instance, while the highest fiber diameter was observed in Group 2, the sample in Group 3 had the lowest fiber diameter. The meltblown process as such is sensitive to interactions of process conditions. Therefore, the effect of all process conditions should be taken into account together, and these conditions should be kept in balance to produce melt-blown fibers with desired fiber diameters.

Fiber Diameter Distributions

Typical fiber diameter distributions for some samples are shown in Figures 5(a-c). Whereas such variability and broad distribution in fiber diameters are typical of meltblown fabrics, data in Table 2 show the median fiber diameters of melt-blown microfibers and their distribution types and parameters that are unique to Biax meltblown webs. Previous studies reported that the diameter of meltblown fibers produced by Exxon die followed a log-normal distribution [15,39,40]. In this study, three different distribution types (normal, log-normal, and skewed log-normal) were observed for meltblown fiber diameters (Figure 6). In addition, the distribution types of some fiber diameters were reported as log-normal (A-D) because their distribution followed a log-normal distribution according to only the Anderson-Darling goodness-of-fit test, not the Kolmogorov-Smirnov test.

As can be seen from the data in Table 2, samples having the highest median of fiber diameter in each group followed a normal distribution. Their air pressure and screw speed were 35 kPa and 40 or 50 rpm during the melt blowing process, respectively. It means that when the fiber diameter is higher, it results in a relatively more uniform web structure as far as fiber diameter distribution is concerned. Barilovits [34] also observed the same tendency during the melt blowing study. Moreover, the skewed log-normal distribution was found in the samples which have fiber diameter close to 1 μm and produced at 20 rpm screw speed.

Whereas wider fiber diameter distribution is likely to produce relatively less uniform web structure, with higher

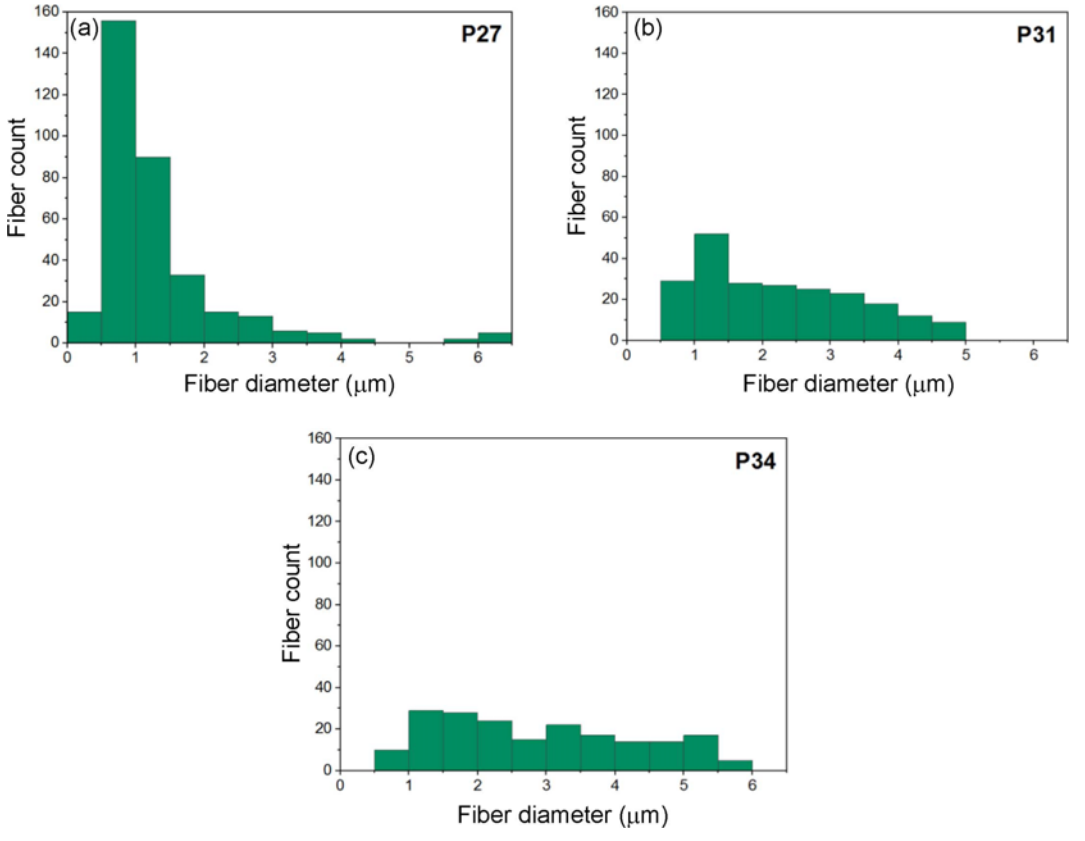

Figure 5. Fiber diameter distributions of some samples in Group 3. (a) P27, (b) P31, and (c) P34 coded samples. The bin size was chosen as 0.5 μm.

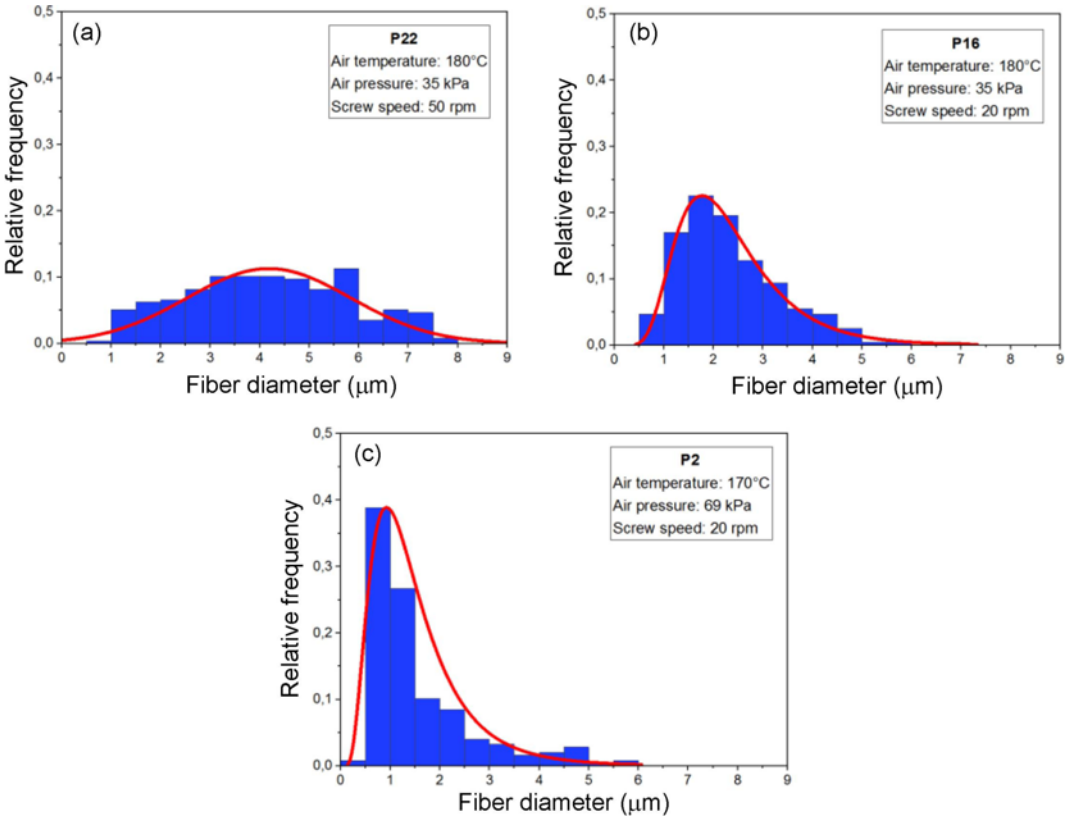

Figure 6. Examples of fiber diameter distributions (a) normal (P22), (b) log-normal (P16), and (c) skewed log-normal (P2). The bin size was chosen as 0.5 μm.

number of finer fibers there is definitely an increase in surface area, and that will result in substantial improvement in properties. Also, based on previous studies, overall fiber diameter distribution in this study is still better, and other properties seem to be not affected to a large extent. In the Exxon type process for comparable webs range of fiber diameters produced might be much wider [41]. These results may be useful in understanding the effect of the combination of conditions on fiber diameter and diameter distribution to produce webs with desired characteristics.

Table 2. Median fiber diameters and distribution parameters

Group	Sample code	Screw speed (rpm)	Air pressure (kPa)	Fiber diameter (μm) (Median)	Distribution	α	μ	σ
Group 1	P1	20	35	1.13	Log-normal	0.02	0.250	0.667
	P2		69	1.15	Skewed log-normal	-	-	-
	P3		103	1.21	Log-normal	0.05	0.183	0.561
	P4	30	35	1.40	Log-normal	0.05	0.399	0.617
	P5		69	1.17	Log-normal(A-D)	0.01	0.295	0.584
	P6		103	1.18	Log-normal	0.05	0.187	0.464
	P7	40	35	1.76	Log-normal	0.05	0.571	0.568
	P8		69	1.30	Log-normal	0.05	0.296	0.500
	P9		103	1.15	Log-normal	0.02	0.186	0.488
	P10	50	35	2.18	Normal	0.02	2.251	1.139
	P11		69	1.44	Log-normal	0.05	0.402	0.507
	P12		103	1.40	Log-normal	0.05	0.380	0.426

Table 2. Continued

Group	Sample code	Screw speed (rpm)	Air pressure (kPa)	Fiber diameter (μm) (Median)	Distribution	α	μ	σ
Group 2	P13	20	35	1.52	Log-normal	0.05	0.472	0.634
	P14		69	1.17	Log-normal	0.05	0.222	0.551
	P15		103	1.03	Log-normal	0.05	0.069	0.484
	P16	30	35	2.13	Log-normal	0.05	0.762	0.436
	P17		69	1.49	Log-normal	0.05	0.435	0.466
	P18		103	1.28	Log-normal	0.01	0.291	0.455
	P19	40	35	2.95	Normal	0.05	3.112	1.345
	P20		69	1.75	Log-normal	0.05	0.593	0.508
	P21		103	1.60	Log-normal	0.05	0.512	0.463
	P22	50	35	4.18	Normal	0.05	4.186	1.657
	P23		69	1.81	Log-normal	0.05	0.612	0.472
	P24		103	1.76	Log-normal	0.05	0.570	0.499
Group 3	P25	20	35	1.23	Log-normal	0.02	0.297	0.634
	P26		69	0.97	Log-normal	0.01	0.049	0.617
	P27		103	1.03	Skewed log-normal	-	-	-
	P28	30	35	1.89	Log-normal	0.05	0.590	0.508
	P29		69	1.25	Log-normal	0.05	0.247	0.467
	P30		103	0.97	Log-normal(A-D)	0.01	0.011	0.414
	P31	40	35	2.03	Log-normal	0.05	0.665	0.555
	P32		69	1.31	Log-normal	0.05	0.284	0.428
	P33		103	0.97	Log-normal(A-D)	0.01	0.066	0.433
	P34	50	35	2.72	Normal	0.02	2.917	1.417
	P35		69	1.34	Log-normal	0.01	0.375	0.469
	P36		103	1.09	Log-normal	0.05	0.120	0.439
Group 4	P37	20	35	1.31	Log-normal(A-D)	0.05	0.396	0.585
	P38		69	1.30	Log-normal	0.05	0.301	0.599
	P39		103	1.09	Log-normal	0.01	0.188	0.605
	P40	30	35	1.50	Log-normal	0.05	0.449	0.558
	P41		69	1.13	Log-normal(A-D)	0.01	0.182	0.560
	P42		103	1.11	Log-normal	0.05	0.168	0.554
	P43	40	35	2.43	Normal	0.02	2.508	1.186
	P44		69	1.87	Log-normal	0.05	0.588	0.506
	P45		103	1.45	Log-normal	0.05	0.400	0.470
	P46	50	35	2.41	Normal	0.02	2.649	1.242
	P47		69	1.37	Log-normal	0.05	0.392	0.441
	P48		103	1.22	Log-normal	0.05	0.246	0.422
Group 5	P49	20	35	1.10	Log-normal	0.02	0.234	0.559
	P50		69	0.97	Log-normal(A-D)	0.01	0.123	0.599
	P51		103	0.97	Skewed log-normal	-	-	-
	P52	30	35	1.34	Log-normal	0.05	0.363	0.568
	P53		69	1.13	Log-normal	0.05	0.190	0.618
	P54		103	0.99	Log-normal(A-D)	0.01	0.102	0.520
	P55	40	35	1.48	Log-normal	0.05	0.407	0.551
	P56		69	1.23	Log-normal	0.05	0.274	0.493
	P57		103	1.24	Log-normal	0.02	0.265	0.463
	P58	50	35	2.29	Normal	0.05	2.371	1.191
	P59		69	1.32	Log-normal	0.05	0.324	0.541
	P60		103	0.97	Log-normal	0.01	0.057	0.472

Conclusion

In this study, the effect of most commonly changed process conditions used in a Biax melt blowing process using a commercial meltblown grade polypropylene resin was investigated in detail with respect to fiber diameter and diameter distribution. This investigation showed that air pressure and melt throughput were the predominant parameters that determine fiber diameter like in the traditional melt blowing process. Melt temperature also had an effect to a certain extent, although it did not follow a specific trend. The fiber diameter distribution was dependent on the fiber diameter, being normal at relatively larger diameters and becoming log-normal when finer fibers were produced. In all the cases, the fiber diameter range was fairly narrow, thus allowing the formation of nonwovens with good structure. Therefore, the Biax process might enable the production of fine fiber nonwovens as well as relatively uniform webs under appropriate process conditions, allowing higher productivity and savings in energy and cost associated with high-pressure hot air. Further studies are being conducted to determine several performance properties of these meltblown webs and will shed more light on this process.

References

1. M. Wehmann and W. J. G. McCulloch in "Polypropylene", 1st ed. (J. Karger-Kocsis Ed.), Vol. 2, pp.415-420, Springer Science+Business Media, Dordrecht, 1999.
2. R. Uppal, G. Bhat, C. Eash, and K. Akato, *Fiber. Polym.*, **14**, 660 (2013).
3. M. A. Hassan, B. Y. Yeom, A. Wilkie, B. Pourdeyhimi, and S. A. Khan, *J. Membr. Sci.*, **427**, 336 (2013).
4. D. Zhang, C. Sun, and H. Song, *J. Appl. Polym. Sci.*, **94**, 1218 (2004).
5. R. R. Hegde and G. S. Bhat, *J. Appl. Polym. Sci.*, **115**, 1062 (2010).
6. E. C. A. Schwarz, *U. S. Patent,* 5476616 (1995).
7. R. Zhao, *A Paper for Insight,* Austin, Texas, Oct 10-14, 2004.
8. M. A. Hassan, S. A. Khan, and B. Pourdeyhimi, *J. Appl. Polym. Sci.*, **133**, 42998 (2016).
9. M. Jafari, Ph. D. Dissertation, NCSU, Raleigh, North Carolina, 2017.
10. H. M. Krutka, R. L. Shambaugh, and D. V. Papavassiliou, *Ind. Eng. Chem. Res.*, **44**, 8922 (2005).
11. Kasen Nozzle, "Meltblown", Available at https://www.kasen.co.jp/english/product/nonwoven-production-part/meltblown-nozzle.php (Accessed February 3, 2020).
12. Biax-Fiberfilm Corporation, "Meltblown Systems", Available at https://www.biax-fiberfilm.com/meltblown-systems (Accessed April 3, 2020).
13. H. Yin, Z. Yan, and R. R. Bresee, *Int. Nonwovens J.*, **8**, 60 (1999).
14. T. Chen, X. Wang, and X. Huang, *Text. Res. J.*, **75**, 76 (2005).
15. C. J. Ellison, A. Phatak, D. W. Giles, C. W. Macosko, and F. S. Bates, *Polymer,* **48**, 3306 (2007).
16. K. C. Dutton, *J. Text. Appar. Technol. Manag.*, **6**, 1 (2008).
17. K. Duran, D. Duran, G. Oymak, K. Kılıç, E. Öncü, and M. Kara, *Tekst. Konfeksiyon,* **23**, 136 (2013).
18. Y. Yesil and G. S. Bhat, *Int. J. Cloth. Sci. Tech.,* **28**, 780 (2016).
19. S. Fakhimi, Ph. D. Dissertation, NCSU, Raleigh, North Carolina, 2017.
20. Y. Lee and L. C. Wadsworth, *Polymer,* **33**, 1200 (1992).
21. R. R. Bresee and U. A. Qureshi, *J. Eng. Fibers Fabr.*, **1**, 32 (2006).
22. Y. Yesil and G. S. Bhat, *J. Text. Inst.*, **108**, 1035 (2017).
23. E. M. Moore, D. V. Papavassiliou, and R. L. Shambaugh, *Int. Nonwovens J.*, **13**, 43 (2004).
24. W. Han, X. Wang, and G. S. Bhat, *J. Nanomater. Mol. Nanotechnol.,* **2**, 1 (2013).
25. R. R. Bresee and W. C. Ko, *Int. Nonwovens J.,* **12**, 21 (2003).
26. R. Nayak, I. L. Kyratzis, Y. B. Truong, R. Padhye, and L. Arnold, *J. Text. Inst.*, **106**, 629 (2015).
27. M. Guo, H. Liang, Z. Luo, Q. Chen, and W. Wei, *Fiber. Polym.*, **17**, 257 (2016).
28. T. Ishikawa, Y. Ishii, Y. Ohkoshi, and K. H. Kim, *Text. Res. J.*, **89**, 1734 (2019).
29. T. Chen and X. Huang, *Text. Res. J.*, **73**, 651 (2003).
30. T. Chen, X. Wang, and X. Huang, *Text. Res. J.*, **74**, 1018 (2004).
31. Y. Pu, J. Zheng, F. Chen, Y. Long, H. Wu, Q. Li, S. Yu, X. Wang, and X. Ning, *Polymers,* **10**, 959 (2018).
32. R. Zhao, *Int. Nonwovens J.*, **14**, 19 (2005).
33. H. M. Krutka, R. L. Shambaugh, and D. V. Papavassiliou, *Ind. Eng. Chem. Res.*, **45**, 5098 (2006).
34. S. Barilovits, Ph. D. Dissertation, NCSU, Raleigh, North Carolina, 2018.
35. B. Dodson, P. C. Hammett, and R. Klerx, "Probabilistic Design for Optimization and Robustness for Engineers", 1st ed., John Wiley & Sons, West Sussex, 2014.
36. K. Krishnamoorthy, "Handbook of Statistical Distributions with Applications", 2nd ed., CRC Press, Boca Raton, Florida, 2016.
37. E. L. Crow and K. Shimizu, "Lognormal Distributions: Theory and Applications", Vol. 88, Marcel Dekker, New York, 1987.
38. Q. Y. Xu and Y. M. Wang, *Adv. Mater. Res.*, **650**, 78 (2013).
39. X. Wang and Q. Ke, *Polym. Eng. Sci.*, **46**, 1 (2006).
40. D. H. Tan, C. Zhou, C. J. Ellison, S. Kumar, C. W. Macosko, and F. S. Bates, *J. Non-Newtonian Fluid Mech.*, **165**, 892 (2010).
41. R. L. Shambaugh, *Ind. Eng. Chem. Res.,* **27**, 2363 (1988).